

Olefin Metathesis over Heterogeneous Catalysts: Interfacial Interaction between Mo Species and a H β -Al₂O₃ Composite Support

Xiujie Li, Weiping Zhang,* Shenglin Liu, Longya Xu, Xiuwen Han, and Xinhe Bao*

State Key Laboratory of Catalysis, Dalian Institute of Chemical Physics, Chinese Academy of Sciences, 457 Zhongshan Road, Dalian 116023, China

Received: November 6, 2007; In Final Form: December 18, 2007

The effect of molybdenum content on the structure and performance of Mo/H β -Al₂O₃ catalysts in olefin metathesis was examined. The optimal performance was obtained with a catalyst of 4–6 wt % Mo on a composite support of 70% H β zeolite and 30% Al₂O₃. The interfacial interaction between the Mo species and the H β -Al₂O₃ composite support was carefully studied by X-ray diffraction (XRD), N₂ adsorption, and multinuclear magic-angle spinning nuclear magnetic resonance (MAS NMR) spectroscopy. XRD and N₂ adsorption results indicate that some interactions may occur between the Mo species and the composite support during the sample preparation. ²⁷Al and ²⁹Si MAS NMR spectra show that this kind of interaction becomes more severe and leads to the dealumination of the framework and subsequent appearance of aluminum molybdate with increasing Mo loadings. Two-dimensional ²⁷Al MQ MAS NMR spectra further demonstrate that the framework Al on H β zeolite at the specific T sites could be preferentially extracted upon Mo loading, which may result in the appropriate Brønsted acidity on the support as evidenced by the quantitative ¹H MAS NMR measurements. A moderate interaction of Mo species with the support and the proper acidity may be advantageous for the cross-metathesis of ethene and 2-butene to propene over heterogeneous catalysts.

Introduction

Olefin metathesis is one of the most important organic reactions discovered in the past 40 years, and it opens up a new route to many important chemicals.¹ The 2005 Nobel Prize in Chemistry was awarded to Chauvin, Grubbs, and Schrock for their development of homogeneous catalysts for olefin metathesis.^{2–4} Heterogeneous catalysts for this reaction will be of great interest because of easy separation, good persistence, and recyclability.¹ Many supported transition-metal compounds can catalyze olefin metathesis, and the most successful ones are those based on Re, W, and Mo.⁵ Usually these metal oxide catalysts are supported on high surface area silica or alumina. Among them, alumina is the most popular support for molybdenum-based metathesis catalysts, and several studies have also dealt with amorphous silica–alumina (ASA) supports, which showed better performance than the single support.^{6,7} Recently our laboratory reported Mo loaded on a H β -Al₂O₃ composite support exhibited high activity in the metathesis of ethene and 2-butene to propene.⁸ This provides an alternative way to meet the increasing demand of propene in the chemical world. While Mo/H β catalyst showed poor activity in this reaction, there is strong interaction between Mo species and H β zeolite, which leads to the appearance of aluminum molybdate.⁹ Therefore, the catalytic performance depends strongly on the nature of the Mo species and the support. Clarification of the interaction between molybdenum oxide and the support is also important for shedding light on the function mechanism of the catalysts.

It is well-known that multinuclear solid-state magic-angle spinning nuclear magnetic resonance (MAS NMR) is a powerful tool for studying the local structures of zeolites and other solid catalysts.^{10,11} Framework and nonframework aluminum species

can be discriminated by ²⁷Al MAS NMR spectra. Two-dimensional ²⁷Al MQ MAS NMR spectra make it possible to remove the anisotropic line broadening and identify the distribution of Al sites by the isotropic projection.¹² In this study, H β -Al₂O₃ was used as the composite support, and different Mo loading catalysts were prepared by the impregnation method. A combination of X-ray diffraction (XRD), N₂ adsorption, ²⁷-Al MAS NMR, two-dimensional ²⁷Al MQ MAS NMR, ²⁹Si MAS NMR, and ¹H MAS NMR was performed to identify some of the chemical species when Mo is present within the composite support. This may be related to the performance of Mo/H β -Al₂O₃ catalysts in the metathesis reaction of ethene and 2-butene to propene.

Experimental Section

Catalyst Preparation and Evaluation. The H β and γ -Al₂O₃ composite support was prepared by extruding a mixture of γ -Al₂O₃ and H β zeolite (Si/Al = 15 provided by Fushun Petroleum Co., China) powder into strips with a diameter of about 2 mm. The support was designed as HB-30Al, which meant the concentration of alumina in the support was 30 wt %. As shown previously,¹³ this is the best support that we used in the olefin metathesis reaction. The composite support was ground to 16–32 mesh after calcination at 500 °C for 2 h. Catalysts with different Mo loadings were prepared by wet impregnation of the H β -Al₂O₃ strips with an aqueous solution of (NH₄)₆Mo₇O₂₄·4H₂O, then dried at 120 °C, and finally calcined at 680 °C for 2 h. The catalysts were denoted as *n*Mo/HB-30Al, where *n* (wt %) stands for the concentration of Mo atoms in the catalysts during preparation. The real Mo contents were checked by XRF and are listed in Table 1.

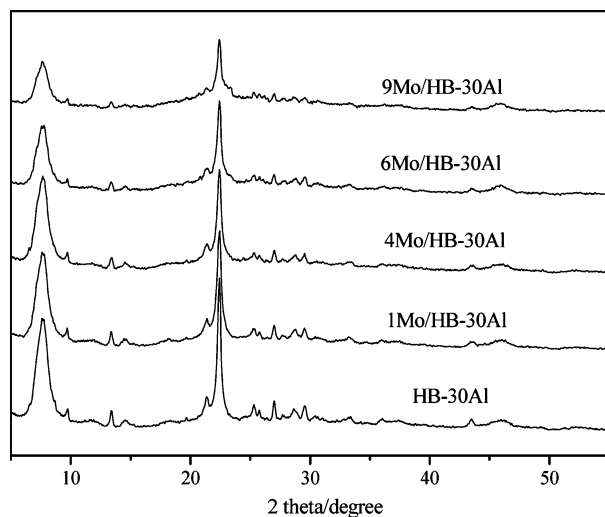
The catalysts (~2.0 g) were tested in a fixed-bed flow microreactor of 10 mm diameter.⁹ After activation for 1 h at

* To whom correspondence should be addressed. Fax: +86-411-8469 4447. E-mail: wpzhang@dicp.ac.cn (W.Z.); xhbao@dicp.ac.cn (X.B.).

TABLE 1: Texture Properties, Relative Crystallinities, Si/Al Ratios, and Brønsted Site Concentrations of H β -Alumina Composite Supports with Different Mo Loadings

sample	HB-30Al	1Mo/HB-30Al	4Mo/HB-30Al	6Mo/HB-30Al	9Mo/HB-30Al
Mo content ^a (%)	0	1.1	4.0	6.2	10.2
relative crystallinity ^b (%)	100	80	68	60	42
BET surface area (m ² /g)	483	403	376	309	241
pore volume (mL/g)	0.45	0.42	0.40	0.28	0.24
framework Si/Al ratio ^c	17	20	28	32	42
C _B ^d (μ mol/g)	235	215	151	105	70

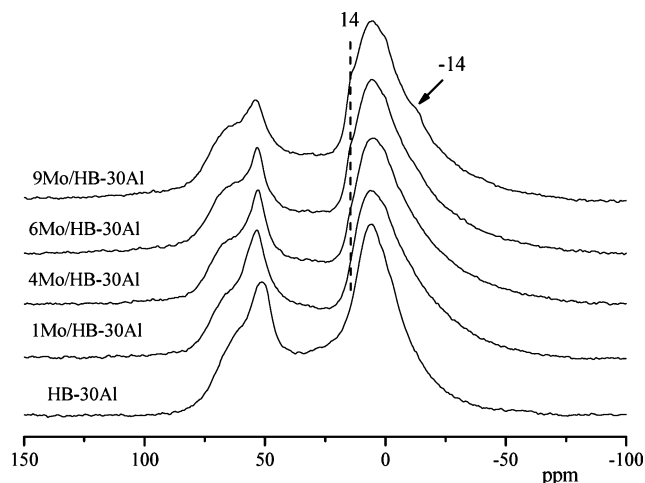
^a Determined by X-ray fluorescence spectroscopy. ^b Determined by XRD patterns, and the intensity of the signal at $2\theta = 22.4^\circ$ was used to evaluate the crystallinity of the β zeolite. ^c Framework Si/Al ratio of H β zeolite in the composite support determined by ²⁹Si MAS NMR spectra. ^d The concentration of Brønsted acidic sites was determined by quantitative analysis of ¹H MAS NMR spectra.

**Figure 1.** XRD patterns of H β -alumina composite supports with different Mo loadings.

550 °C under nitrogen to remove the moisture, they were cooled to the reaction temperature at 120 °C. The reaction products were analyzed by a Shimadzu GC-8A gas chromatograph with an FID detector. The conversion of ethene and 2-butene was calculated on the basis of the carbon number using methane and butane as the internal standards.

XRD and N₂ Adsorption Measurements. X-ray diffraction patterns were obtained at room temperature on a Rigaku D/Max-RB diffractometer using Cu K α radiation. Powder diffractograms of the samples were recorded over a range of 2θ values from 5° to 50° under the conditions of 40 kV and 100 mA at a scanning rate of 8 deg/min. The integrated intensity of the signal at $2\theta = 22.4^\circ$ was used to evaluate the crystallinity of the β zeolites.¹⁴ Nitrogen sorption experiments were performed at -196 °C on an ASAP 2000 system in the static measurement mode. Samples were outgassed at 350 °C for 10 h before the measurements. Specific surface areas were calculated by the BET method, and the pore volume was determined by N₂ adsorption at a relative pressure of 0.98.

NMR Measurements. All NMR spectra were recorded on Varian Infinity plus-400 spectrometer. ²⁷Al MAS NMR experiments were carried out using a 2.5 mm MAS NMR probe with a spinning rate of 25 kHz. Chemical shifts were referenced to (NH₄)Al(SO₄)₂·12H₂O at -0.4 ppm as a secondary reference. The spectra were accumulated for 1024 scans with a $\pi/12$ flip angle and a 2 s pulse delay. For a quantitative comparison, all samples were weighted and hydrated completely in a desiccator with saturated NH₄NO₃ solution, and the spectra were calibrated by measuring a known amount of (NH₄)Al(SO₄)₂·12H₂O under the same conditions.^{15,16} ²⁷Al 3Q MAS NMR experiments were performed using a three-pulse sequence incorporating a z-filter at a spinning speed of 25 kHz with a 2.5 mm probe.¹⁷ An rf

**Figure 2.** ²⁷Al MAS NMR spectra of H β -alumina composite supports with different Mo loadings.

field of 200 kHz was used for the creation (0Q \rightarrow ± 3 Q) and the first conversion (± 3 Q \rightarrow 0Q) pulses. For the last conversion step (0Q \rightarrow ± 1 Q), which was the central transition selective soft 90° pulse, an rf field of 18 kHz was used. A 2D Fourier transformation followed by a shearing transformation gave a pure absorption mode 2D contour plot.^{18–20} The second-order quadrupolar effect (SOQE) and isotropic chemical shift (δ_{iso}) values were calculated according to the procedures in ref 19. ²⁹Si MAS NMR spectra with high-power proton decoupling were recorded at 79.4 kHz using a 7.5 mm MAS probe with a spinning rate of 4 kHz. 4,4-Dimethyl-4-silapentanesulfonate sodium salt (DSS) was used as the chemical shift reference for ²⁹Si MAS NMR spectroscopy. A total of 1024 scans were accumulated with a $\pi/4$ pulse width of 1 μ s and a 4 s recycle delay. Before the ¹H MAS NMR measurements, the samples were dehydrated at 400 °C and a pressure below 10⁻² Pa for 20 h to remove the water moisture. ¹H MAS NMR spectra were collected at 399.9 MHz using a single-pulse sequence with a $\pi/4$ pulse and a 4 s recycle delay with a spinning speed of 10 kHz. Chemical shifts were referenced to DSS. For the quantitative determination of the ¹H MAS NMR results, all samples were weighed, and the spectra were calibrated by measuring a known amount of 1,1,1,3,3,3-hexafluoro-2-propanol performed in the same conditions.¹⁶ The Dmfit software was employed for deconvolution using fitted Gaussian-Lorentzian line shapes.²¹

Results and Discussion

XRD and N₂ Adsorption Data. XRD patterns of HB-30Al composites support with different Mo loadings are shown in Figure 1. It can be seen that typical diffraction peaks of H β zeolite are present on the composite support.¹⁴ The weak and broad line assigned to alumina at 46° is also clearly observed. As listed in Table 1, the relative crystallinity decreases to 42%

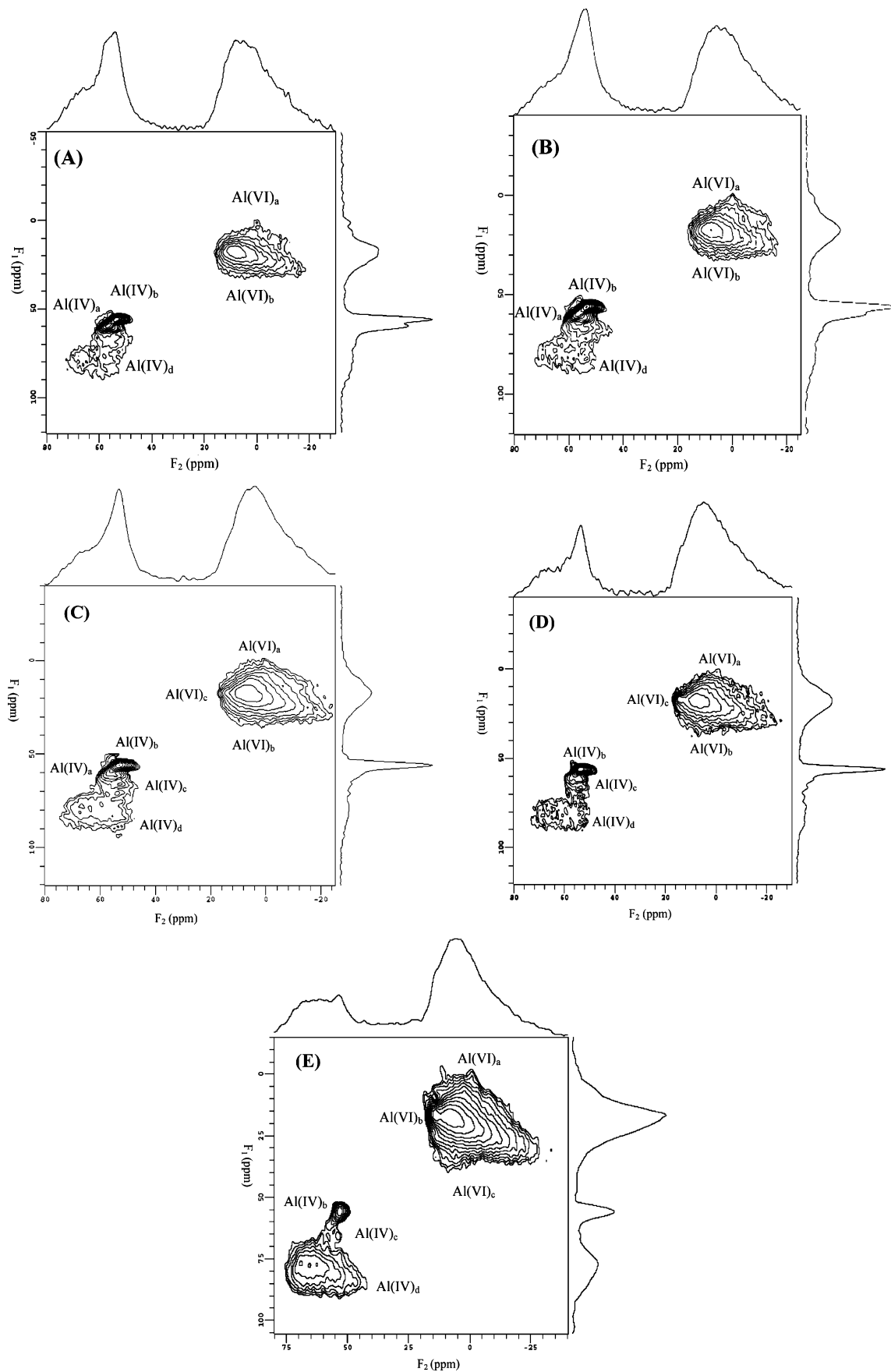


Figure 3. Two-dimensional ^{27}Al MQ MAS NMR spectra of the samples: (A) HB-30Al, (B) 1Mo/HB-30Al, (C) 4Mo/HB-30Al, (D) 6Mo/HB-30Al, (E) 9Mo/HB-30Al. The corresponding ^{27}Al MAS NMR spectrum is given on top of the MQ MAS plot. The F_1 projection is the pure isotropic spectrum.

TABLE 2: NMR Parameters Determined from ^{27}Al MQ MAS NMR for $n\text{Mo}/\text{HB}-30\text{Al}$ Samples

sample	Al(IV) _a	Al(IV) _b	Al(IV) _c	Al(IV) _d	Al(VI) _a	Al(VI) _b	Al(VI) _c
HB-30Al	58.4 ^a (1.8) ^b	54.8 (1.6)		73.2 (3.5)	0.9 (1.4)	13.9 (3.2)	
1Mo/HB-30Al	59.1 (1.9)	55.1 (1.6)		72.7 (3.5)	1.0 (1.3)	13.8 (3.3)	
4Mo/HB-30Al	58.8 (2.1)	54.7 (1.7)	58.3 (3.2)	73.3 (3.6)	0.9 (1.4)	13.1 (3.3)	15.8 (1.6)
6Mo/HB-30Al	59.5 (1.9)	54.8 (1.6)	58.4 (3.0)	73.1 (3.6)	0.9 (1.4)	13.3 (3.2)	15.6 (1.5)
9Mo/HB-30Al		54.7 (1.7)	59.8 (3.6)	72.7 (3.8)	1.0 (1.5)	13.4 (3.2)	15.2 (1.5)

^a δ_{iso} (ppm). ^b P_{Q} (MHz).

on Mo loading up to 9.0 wt %, indicating that Mo species obviously interact with the composite support. There is no XRD evidence for the presence of a crystalline MoO_3 phase. This suggests that the Mo species must be dispersed in some form over the support. However, we cannot rule out the formation of disordered MoO_3 or $\text{Al}_2(\text{MoO}_4)_3$ phases, which cannot be detected by XRD. Table 1 also lists the BET surface areas and pore volumes of Mo/HB-30Al samples. It is found that the incorporation of Mo species causes a loss in the total surface area and pore volume of the support, implying that the interaction between the Mo species and the composite support causes a partial collapse of the pore network during the sample preparation.

^{27}Al MAS and Two-Dimensional MQ MAS NMR. ^{27}Al MAS NMR has been widely used to determine the coordination and local structure of specific aluminum species in zeolites and alumina since different ^{27}Al sites can be readily resolved by one-dimensional ^{27}Al MAS NMR combined with two-dimensional MQ MAS NMR spectroscopy.²² Figure 2 shows the one-dimensional ^{27}Al MAS NMR spectra of $\text{H}\beta$ -alumina composite supports with different Mo loadings. Two peaks in the tetrahedral region were observed in the ^{27}Al MAS NMR spectrum of the support. The signal at 54 ppm is assigned to framework tetrahedral aluminum in $\text{H}\beta$ zeolite.^{9,23} The broad one centered at ca. 64 ppm comes from the four-coordinated aluminum in alumina.²⁴ In the octahedral region, only a broad signal centered at ca. 5 ppm is observed, which can be attributed to the six-coordinated aluminum in alumina. This signal is also overlapped with that from the nonframework Al in $\text{H}\beta$ zeolite. After Mo loading, the intensity of the peak at 54 ppm decreases accordingly. When Mo loading is up to 9.0 wt %, two new peaks appear at -14 and +14 ppm, corresponding to the nonhydrated and hydrated forms of the aluminum molybdate phase.^{9,25} Therefore, there can be a chemical reaction between the Mo species and the support, which leads to the appearance of aluminum molybdate at higher Mo loadings. However, it is difficult to separate the contribution of aluminum with different isotropic shifts and quadrupolar coupling constants in the one-dimensional ^{27}Al MAS NMR spectra; one possibility is to use the two-dimensional multiple quantum technique.¹⁹

The ^{27}Al MQ MAS NMR spectrum of the $\text{H}\beta$ -alumina composite support is shown in Figure 3A. Shearing the projection of the 2D frequency domain along the δ_{F1} axis gives the purely isotropic spectrum free of second-order quadrupolar broadening. At least three different contributions are distinguished in the 50–70 ppm region attributed to tetrahedrally coordinated aluminum species. The Al(IV)_a and Al(IV)_b signals come from the framework tetrahedral Al in $\text{H}\beta$ zeolite similar to that previously reported in ref 23. Table 2 lists the isotropic chemical shifts δ_{iso} and quadrupolar parameters P_{Q} . It can be deduced from Figure 3A that at least two groups of crystallographically distinct T sites exist in the $\text{H}\beta$ framework. The crystallographic T sites corresponding to the tetrahedral peak Al(IV)_b are more populated than the T sites corresponding to the tetrahedral peak Al(IV)_a for the $\text{H}\beta$ -alumina composite support. The ratio of the two is, however, a function of the Mo

loading. In the octahedral region, a strong peak corresponding to octahedral Al species in alumina is observed and designated as Al(VI)_b. In addition, the isotropic projection reveals a small line (Al(VI)_a) at 0 ppm indicating the presence of nonframework Al in $\text{H}\beta$ zeolite.

After introduction of 1.0 wt % Mo, the Al(IV)_a and Al(IV)_b signals can still be resolved in Figure 3B while the relative ratio $I_{\text{Al(IV)a}}/I_{\text{Al(IV)b}}$ decreases. Therefore, the Mo species interact preferentially with the specific T sites Al(IV)_a of $\text{H}\beta$ zeolite in the composite support. When the Mo loading is as high as 4.0 wt %, a new signal, Al(IV)_c, appears. From its position in the isotropic dimension of 3Q MAS NMR spectra in Figure 3C, Al(IV)_c should be regarded as that from four-coordinated aluminum species. This peak represents only a small fraction of the total spectral intensity but experiences a large quadrupolar interaction ($P_{\text{Q}} = 3.2$ MHz) as summarized in Table 2. This large anisotropic quadrupolar broadening makes it difficult to identify in the usual ^{27}Al MAS NMR spectra; however, it is clearly noticeable in the isotropic F_1 projection. This species may be a locally distorted aluminum atom associated with a defective site in the $\text{H}\beta$ framework, which could be generated by high-temperature calcination, acid leaching, or steam treatment.^{26,27} In our case, it is the introduction of Mo species that leads to the formation of such a third Al(IV)_c at the expense of Al(IV)_a. The decrease in the amount of the Al(IV)_a species further indicates that Mo species remove preferentially the aluminum atoms from the crystallographic position represented by Al(IV)_a. At the same time a new signal, Al(VI)_c, is seen in the octahedral region besides Al(VI)_a and Al(VI)_b. In accordance with the one-dimensional ^{27}Al MAS NMR spectra, this signal is assigned to the hydrated form of aluminum molybdate. Introduction of 6.0 wt % Mo leads to a more pronounced Al(IV)_c peak and the loss of the tetrahedrally coordinated aluminum Al(IV)_a species. Figure 3E displays the ^{27}Al MQ MAS NMR spectra of the 9Mo/HB-30Al sample. Compared with 6.0 wt % Mo loading, the peak of aluminum molybdate is more evident, suggesting that the Mo species interact strongly with the support to produce more $\text{Al}_2(\text{MoO}_4)_3$ upon Mo loading. In the meantime not only were the Al(IV)_a species fully removed from the $\text{H}\beta$ zeolite, but also part of the Al(IV)_b aluminum species were extracted from the framework. As indicated in Table 2, the Al(IV)_c species in the tetrahedral region experiences a larger quadrupolar interaction when the Mo loading is up to 9.0 wt %. Therefore, different crystallographic T sites on $\text{H}\beta$ zeolite have different resistance abilities for Mo loading. The Al(IV)_a species may interact more easily than the Al(IV)_b species with the Mo species so that it can be extracted readily from the framework of $\text{H}\beta$ zeolite. This is probably because the Al(IV)_a species experiences a larger quadrupolar effect in the tetrahedral region (cf. Table 2).

^{29}Si MAS NMR. The ^{29}Si MAS NMR spectra of $\text{H}\beta$ -alumina composites with different Mo loadings are shown in Figure 4. Three major resonances at around -117, -113, and -107 ppm are observed. The first two lines are attributed to the inequivalent framework sites of the $\text{H}\beta$ zeolite, which correspond to Si(0Al) groupings. The line at -107 ppm is

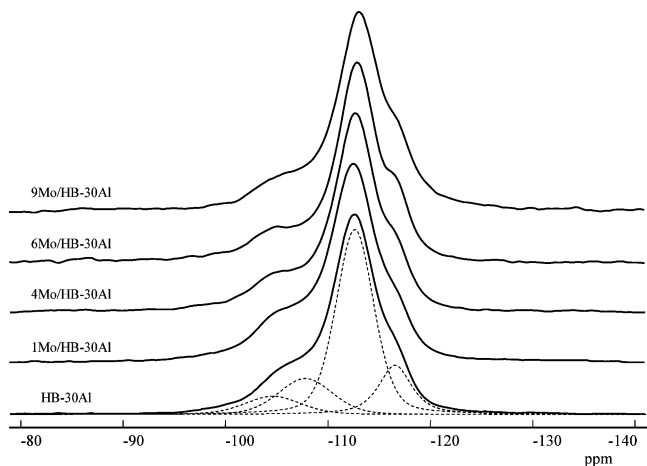


Figure 4. ^{29}Si MAS NMR spectra of $\text{H}\beta$ -alumina composite supports with different Mo loadings.

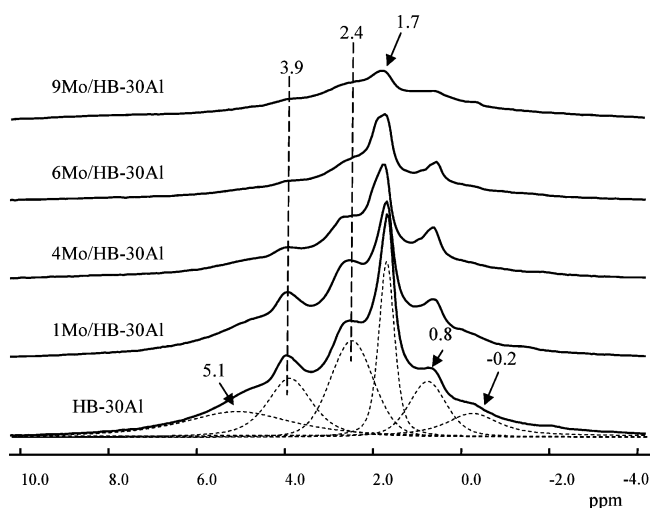


Figure 5. ^1H MAS NMR spectra of $\text{H}\beta$ -alumina composite supports with different Mo loadings. The spinning rate was 10 kHz, and 200 single-pulse scans were accumulated.

supposed to come from the contribution of Si(1Al) groupings. The downfield peak at around -103 ppm is associated with Si atoms in $\text{Si}(\text{OSi})_3\text{OH}$ environments.²⁸ As shown in our previous study,⁹ the line at -107 ppm is supposed to come from the contribution of Si(1Al) groupings. The framework Si/Al ratio can be calculated by deconvolution of the ^{29}Si MAS NMR spectra, and the results are listed in Table 1. It can be seen that the framework Si/Al ratio increases with increasing Mo loading. This fact further proves that introduction of Mo species causes the dealumination of the $\text{H}\beta$ framework, which is in accordance with the above results from ^{27}Al MAS NMR.

^1H MAS NMR. High-resolution ^1H MAS NMR is a useful and direct method to characterize the Brønsted acidic sites in catalysts. Figure 5 shows the ^1H MAS NMR spectra of $n\text{Mo}/\text{HB}-30\text{Al}$ catalysts. Due to the addition of alumina into the support, the spectrum of $\text{H}\beta$ -alumina composites is a little more complex than that of $\text{H}\beta$ zeolite.⁹ As demonstrated, the signal at about -0.2 ppm is assigned to the basic hydroxyls in alumina; the peak at ca. 2.4 ppm may contain the contribution of nonframework AlOH in $\text{H}\beta$ zeolite and the acidic hydroxyls in alumina.^{13,29} Additionally, two other peaks at about 0.8 and 1.7 ppm can be observed, which are respectively attributed to the nonacidic unperturbed extraframework aluminum hydroxyls and silanol groups in $\text{H}\beta$. At the same time the peak at 3.9 ppm could be clearly resolved and should be assigned to the bridging

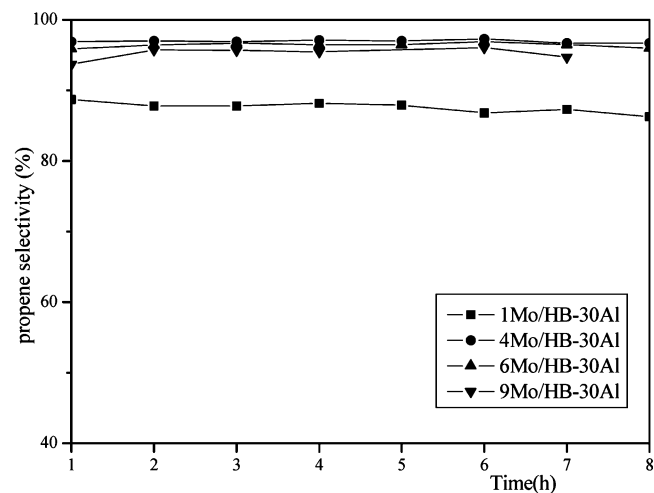
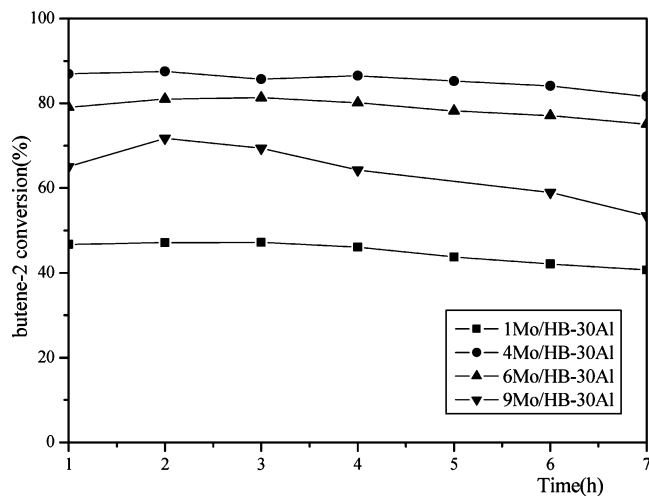


Figure 6. Catalytic conversions and selectivities of $n\text{Mo}/\text{HB}-30\text{Al}$ catalysts with different Mo contents in the metathesis of ethene and 2-butene to propene (reaction temperature 393 K, pressure 1.0 MPa, ethene/2-butene = 3/1, WHSV of ethene 1.2 h^{-1}).

hydroxyl groups, i.e., Brønsted acidic sites in $\text{H}\beta$.³⁰ In the deconvoluted spectra a broad line centered at ca. 5.1 ppm could be identified. It is ascribed to a second Brønsted acidic site interacting electrostatically with the zeolite framework since it could be significantly suppressed after Al irradiation.⁹ Figure 5 illustrates that the total ^1H signal intensity decreases upon Mo loading, and the peaks at -0.2 and 1.7 ppm are preferentially reduced compared to those at 3.9 ppm. This indicates that during the catalyst preparation the Mo species first react with the basic Al hydroxyls and silanols on the surface of the support. A similar prior reaction between basic $\text{Al}-\text{OH}$ and Mo species was also observed on $\text{Mo}/\text{Al}_2\text{O}_3$ samples.³¹ When the Mo loading is as high as 4.0 wt %, the peak intensity of the Brønsted acidic sites is clearly reduced. Quantitative results concerning the amounts of Brønsted acidic sites on the catalysts after Mo loading are reported in Table 1. It is found that the content of Brønsted acidic sites on the support surface obviously decreases as the Mo loading is increased up to 9.0 wt %, indicating that Mo species strongly interact with the framework Al with subsequent dealumination of the framework and loss of Brønsted acidic sites.

Catalytic Performance of Cross-Metathesis of Ethene and 2-Butene to Propene. The catalytic performance of olefin metathesis on $n\text{Mo}/\text{HB}-30\text{Al}$ catalysts, as a function of molybdenum content, is presented in Figure 6. It is clear that 1.0 wt % Mo loading on the $\text{H}\beta$ -alumina composite support

shows the lowest performance; i.e., the 2-butene conversion is 47%, and the propene selectivity is about 87%. When the Mo content increases to 4.0–6.0 wt %, the catalysts show the highest metathesis activity. Under this condition the 2-butene conversion is up to 80% and the propene selectivity is about 95%. At the same time these catalysts have high stability, which show no obvious deactivation within 7 h. With the Mo content further increasing to 9.0 wt %, however, the activity of the catalyst decreases.

When the results from solid-state NMR with the above catalytic performances of Mo/H β -Al₂O₃ are compared, it seems that moderate interaction between Mo species and the H β -Al₂O₃ support is important for the metathesis reaction. The catalyst activity increases with Mo loadings up to 4.0–6.0 wt % because Mo species are the active sites and more Mo species mean more activity. Higher Mo loading leads to a decrease of activity, which may be related to the significant loss of surface area caused by the dealumination of the zeolite framework due to the strong interaction between the Mo species and the support. This kind of interaction will also influence the reducibility of Mo species as shown by our previous H₂-TPR results⁸ and the following formation of the active species molybdenum carbene. At the same time the catalyst acidity is also crucial for heterogeneous olefin metathesis as reviewed by Andreini et al.³³ In our case, when the Mo content is lowered to 1.0 wt %, more Brønsted acidic sites are present on the catalyst as evidenced by ¹H MAS NMR. This may enhance the olefin oligomerization and/or isomerization side reactions and result in lower metathesis activity as evidenced by our recent ongoing study. Initial interaction of the Mo species with the nonacidic hydroxyl groups on the support may also lead to the formation of less active precursor in the metathesis reaction as suggested by Mol et al.³² When the concentration of Mo is between 4.0 and 6.0 wt %, there exists an appropriate interaction between the Mo species and the support, which preserves the aluminum atoms at specific T sites in H β zeolite; thus, there is moderate Brønsted acidity on the catalysts. This is beneficial for the metathesis reaction although the Mo species are the active centers. The residual Brønsted acidic sites on the catalyst may be involved in the initiation of the metathesis reaction as described by Andreini et al. in the study of Re/Al₂O₃ catalysts.³³ The residual Lewis acid sites may not be necessary because this reaction mechanism may be related to the metal hydride and the subsequent the metal carbene after introduction of olefins as proposed by Laverty et al.³⁴ A high Mo loading of 9.0 wt % results in the dealumination of the support framework, the obvious formation of Al₂(MoO₄)₃ species, and thus less acidity. Such a strong interaction between the Mo species and the support is supposed to be responsible for the poor performance of the catalyst in olefin metathesis reaction.

Conclusions

As demonstrated by XRD and N₂ adsorption measurements, Mo species may interact with the H β -alumina composite support during the sample preparation. ²⁷Al and ²⁹Si MAS NMR spectra show that this kind of interaction is so strong that the framework aluminum could be extracted from H β zeolite, and Al₂(MoO₄)₃ appears when the Mo loading is up to 9.0 wt %. The formation of more Al₂(MoO₄)₃ species may cause the catalyst to become less active for olefin metathesis. Two-dimensional ²⁷Al MQ MAS NMR spectra show the gradual

extraction of framework Al species at specific T sites on H β zeolite upon Mo loading. Quantitative ¹H MAS NMR spectra indicate an appropriate Brønsted acidity when the Mo loading is 4.0–6.0 wt %. A moderate interaction of Mo species with the support and the proper acidity may be advantageous for the metathesis of ethene and 2-butene to propene over heterogeneous catalysts.

Acknowledgment. We are grateful for the financial support of the National Natural Science Foundation of China (Grant Nos. 20403017 and 20773120) and the Ministry of Science and Technology of China through the National Key Project of Fundamental Research (Grant No. 2003CB615806). We thank the anonymous reviewer for the fruitful discussions and suggestions during the revision.

References and Notes

- Mol, J. C. *J. Mol. Catal. A* **2004**, *213*, 39.
- Chauvin, Y. *Angew. Chem., Int. Ed.* **2006**, *45*, 3740.
- Grubbs, R. H. *Angew. Chem., Int. Ed.* **2006**, *45*, 3760.
- Schrock, R. R. *Angew. Chem., Int. Ed.* **2006**, *45*, 3748.
- Ivin, K. J.; Mol, J. C. *Olefin metathesis and metathesis polymerization*, 2nd ed.; Academic Press: San Diego, 1996.
- Rajagopal, S.; Marini, H. J.; Marzari, J. A.; Miranda, R. *J. Catal.* **1994**, *147*, 417.
- Hu, B.; Gay, I. D. *J. Phys. Chem. B* **2001**, *105*, 217.
- Liu, S.; Huang, S.; Xin, W.; Bai, J.; Xie, S.; Xu, L. *Catal. Today* **2004**, *93–95*, 471.
- Li, X.; Zhang, W.; Liu, S.; Han, X.; Xu, L.; Bao, X. *J. Mol. Catal. A* **2006**, *250*, 94.
- Klinowski, J. *Chem. Rev.* **1991**, *91*, 1459.
- Laws, D. D.; Bitter, H. M. L.; Jerschow, A. *Angew. Chem., Int. Ed.* **2002**, *41*, 3096.
- Fernandez, C.; Amoureux, J. P. *Chem. Phys. Lett.* **1995**, *242*, 449.
- Li, X.; Zhang, W.; Liu, S.; Xu, L.; Han, X.; Bao, X. *J. Catal.* **2007**, *250*, 55.
- Eapen, M. J.; Reddy, K. S. N.; Shiralkar, V. P. *Zeolites* **1994**, *14*, 295.
- Kraus, H.; Prins, R. *J. Catal.* **1996**, *164*, 260.
- Muller, M.; Harvey, G.; Prins, R. *Microporous Mesoporous Mater.* **2000**, *34*, 281.
- Amoureux, J.-P.; Fernandez, C.; Steuernagel, S. *J. Magn. Reson., A* **1996**, *123*, 116.
- Smith, M. E.; van Eck, E. R. H. *Prog. Nucl. Magn. Reson. Spectrosc.* **1999**, *34*, 159.
- Rocha, J.; Morais, C. M.; Fernandez, C. *Top. Curr. Chem.* **2004**, *246*, 141.
- Medek, A.; Harwood, J. S.; Frydman, L. *J. Am. Chem. Soc.* **1995**, *117*, 12779.
- Massiot, D.; Fayon, F.; Capron, M.; King, I.; Le Calve, S.; Alonso, B.; Durand, J. O.; Bujoli, B.; Gan, Z. H.; Hoatson, G. *Magn. Reson. Chem.* **2002**, *40*, 70.
- Goldbourt, A.; Madhu, P. K. *Annu. Rep. NMR Spectrosc.* **2005**, *54*, 81.
- van Bokhoven, J. A.; Koningsberger, D. C.; Kunkeler, P.; van Bekkum, H.; Kentgens, A. P. M. *J. Am. Chem. Soc.* **2000**, *122*, 12842.
- Kraus, H.; Muller, M.; Prins, R.; Kentgens, A. P. M. *J. Phys. Chem. B* **1998**, *102*, 3862.
- Zhang, W.; Ma, D.; Han, X.; Liu, X.; Bao, X.; Guo, X.; Wang, X. *J. Catal.* **1999**, *188*, 393.
- Abraham, A.; Lee, S. H.; Shin, C. H.; Hong, S. B.; Prins, R.; van Bokhoven, J. A. *Phys. Chem. Chem. Phys.* **2004**, *6*, 3031.
- Omegna, A.; Vasic, M.; van Bokhoven, J. A.; Pirngruber, G.; Prins, R. *Phys. Chem. Chem. Phys.* **2004**, *6*, 447.
- Perez-Pariente, J.; Sanz, J.; Fornes, V.; Corma, A. *J. Catal.* **1990**, *124*, 217.
- Zhang, W. P.; Sun, M. Y.; Prins, R. *J. Phys. Chem. B* **2002**, *106*, 11805.
- Hunger, M. *Catal. Rev.—Sci. Eng.* **1997**, *39*, 345.
- Jacobsen, C. J. H.; Topsoe, N. Y.; Topsoe, H.; Kellberg, L.; Jacobsen, H. J. *J. Catal.* **1995**, *154*, 65.
- Mol, J. C. *Catal. Today* **1999**, *51*, 289.
- Andreini, A. *J. Mol. Catal.* **1991**, *65*, 359.
- Laverty, D. T.; Rooney, J. J.; Stewart, A. *J. Catal.* **1976**, *45*, 110.